APPLICATION OF OPTIMIZATION TECHNIQUES TO THE DESIGN OF A FLUTTER SUPPRESSION CONTROL LAW FOR THE DAST ARW-2

William M. Adams, Jr., and Sherwood H. Tiffany
NASA Langley Research Center
Hampton, Virginia

OUTLINE

This paper describes the design of a candidate flutter suppression (FS) control law for the symmetric degrees of freedom for the DAST ARW-2 aircraft. The results shown here illustrate the application of several currently employed control law design techniques. Subsequent designs, obtained as the mathematical model of the ARW-2 is updated, are expected to employ similar methods and to provide a control law whose performance will be flight tested. This study represents one of the steps necessary to provide an assessment of the validity of applying current control law synthesis and analysis techniques in the design of actively controlled aircraft. Mathematical models employed in the control law design and evaluation phases are described. The control problem is specified by presenting the flutter boundary predicted for the uncontrolled aircraft and by defining objectives and constraints that the controller should satisfy. A full-order controller is obtained by using Linear Ouadratic Gaussian (LQG) techniques (Refs. 1-4). The process of obtaining an implementable reduced-order controller is described (Refs. 5,6). One example is also shown in which constrained optimization techniques (Refs. 7-11) are utilized to explicitly include robustness criteria within the design algorithm.

- MATHEMATICAL MODELING
- ARW-2 FLUTTER CHARACTERISTICS
- CONTROLLER DESIGN OBJECTIVES AND CONSTRAINTS
- FULL-ORDER CONTROLLER DESIGN
- REDUCED-ORDER CONTROLLER DEFINITION
- MAXIMIZATION OF ROBUSTNESS OF REDUCED-ORDER CONTROLLER

SENSOR SIGNAL INPUTS TO SYMMETRIC FLUTTER SUPPRESSION CONTROL LAW

The symmetric FS control law described here receives a feedback signal obtained by differencing the output of two vertical accelerometers located as shown on the outboard portion of the wing. Antisymmetric contributions are removed by summing signals from each wing semispan. The signal, properly compensated, is fed to each outboard aileron actuator. The objective of the FS design is to determine the compensation required to suppress flutter while satisfying other design criteria such as control power and robustness constraints.

Note that the control law is single-input/single-output (SISO). Furthermore, the sensor signal accentuates the observability of predominantly torsional modes at the expense of predominantly bending modes. It is planned, in a subsequent study, to investigate the benefit of including the sum of the accelerometer outputs as an additional feedback signal.

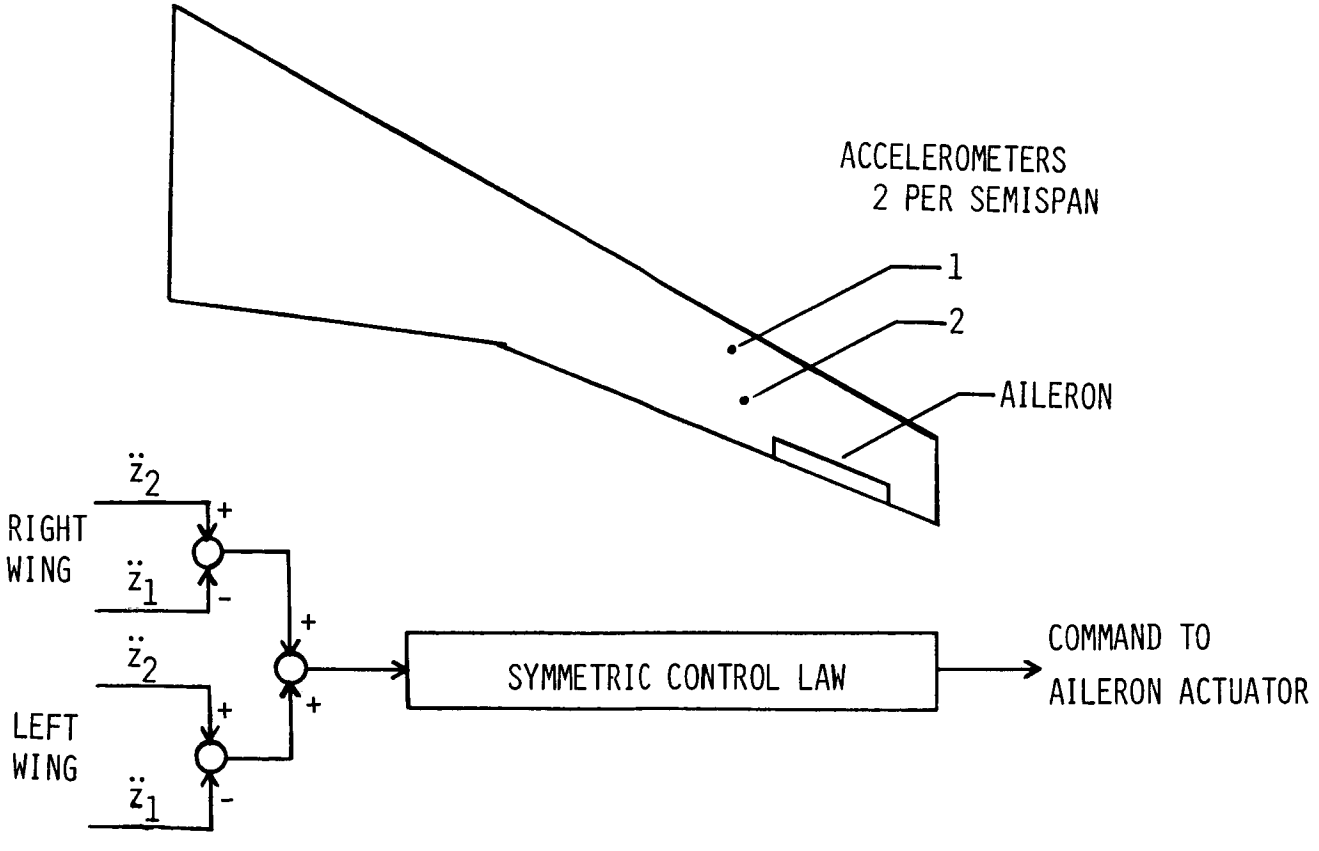

MATHEMATICAL MODELING

Mathematical models were developed using the ISAC (Interaction of Structures, Aerodynamics and Controls, Ref. 12) program. A modal characterization of the aircraft was employed which resulted from performing a free-free vibration analysis with symmetric constraints. Twelve symmetric modes were retained for the modeling: mean-body vertical translation and pitch plus 10 symmetric elastic modes.

Unsteady aerodynamic forces were computed for oscillatory motion by using a doublet lattice technique (Refs. 13,14) for several Mach numbers (M) and, at each Mach number, for a range of reduced frequencies (k). Reduced frequency satisfies the relationship $k = \omega\, b/U$ where b is a reference length (chosen here to be one half the mean aerodynamic chord of the wing), U is airspeed and ω is frequency in rad/sec.

A third-order transfer function representation of the actuator was employed which provided a good fit to its experimentally determined frequency response below a frequency of 300 rad/sec.

Approximate unsteady aerodynamic forces for arbitrary motion were generated in order to obtain a linear, time invariant (LTI) state space model. A least squares curve fit was made, at each Mach number, of the complex matrix of frequency dependent aerodynamic force coefficients, using a matrix function (Refs. 15-19). Constraints were imposed upon the rigid body and gust columns of A_0, A_1 and the C_I matrices which required that the curve fit match the tabular data and its slope at k=0 (Ref. 20). In addition, the column of A_2, corresponding to forces due to gust inputs, was constrained to be zero.

The resulting LTI state space evaluation model was 77th order. (Four lag terms were employed in the s-plane fit and a second-order Dryden representation (Ref. 21) of the gust spectrum was used.)

- MODAL CHARACTERIZATION OF STRUCTURE (2 RIGID BODY AND 10 FREE-FREE ELASTIC MODES)
- DOUBLET LATTICE COMPUTATION OF UNSTEADY AERODYNAMIC FORCES
- 3RD ORDER REPRESENTATION OF ACTUATOR
- S-PLANE APPROXIMATION OF UNSTEADY AERODYNAMICS (4 LAG TERMS)

$$Q = A_0 + A_1 S + A_2 S^2 + \sum_{I=1}^{4} \frac{S\, C_I}{(S + B_I)}$$

- 77 STATE EVALUATION MODEL

DESIGN MODEL

A reduced-order model of the plant was developed in order to lower the cost of the control law design. Only two lag terms were used in the s-plane approximation. Modes with natural frequencies below or near the open-loop flutter frequency which were observed to have little effect upon the flutter characteristics were truncated. Modal residualization (Refs. 3,10,22,23) was employed to retain the static effects of the highest frequency modes. Five modes were retained in the design model, which had a 25th order state space representation (10 vehicle, 10 aerodynamic, 3 actuator, 2 gust).

- TRUNCATE NONCRITICAL MODES IN FLUTTER FREQUENCY RANGE OR BELOW
- REMOVE HIGH-FREQUENCY MODES BY MODAL RESIDUALIZATION
- TWO LAG S-PLANE AERODYNAMIC FORCE APPROXIMATION
- 25 STATE DESIGN MODEL

AMPLITUDE OF SENSOR OUTPUT/CONTROL INPUT TRANSFER FUNCTION

Bode plots of the symmetric signal sent to the controller per unit commanded control input were generated for the analysis and design models. The design model sensor signal amplitude is in good agreement with that of the full-order evaluation model. Phase angle comparisons, not shown, also exhibit excellent agreement at frequencies below 500 rad/sec.

The evaluation model Bode plot was actually generated using the second-order form of the equations of motion. The unsteady aerodynamic forces computed using the doublet lattice technique are in the proper form for this frequency domain analysis. Therefore, no s-plane approximation is needed.

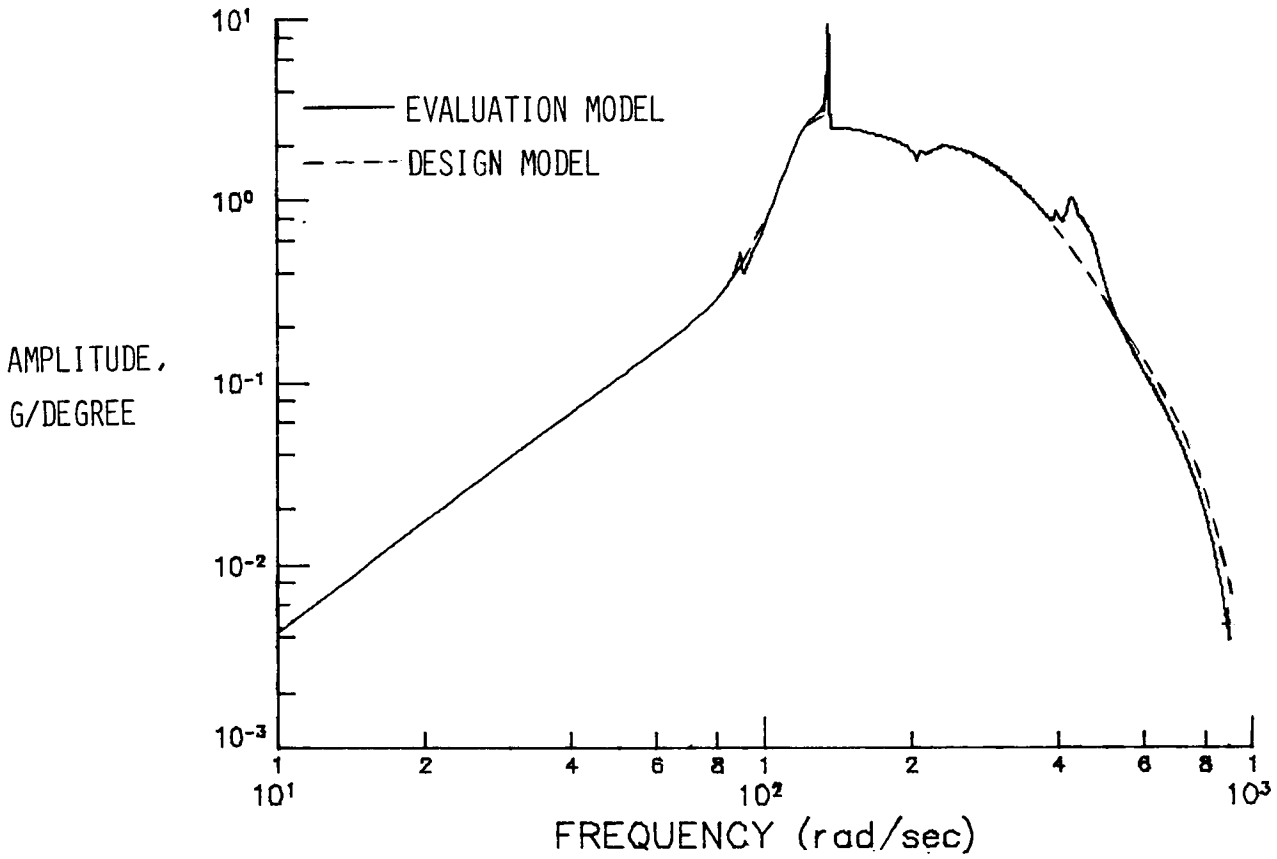

FLUTTER BOUNDARY, FS-OFF; NOMINAL STABILITY MARGIN BOUNDARY
AND FLUTTER BOUNDARY, FS-ON

The predicted flutter boundary (FS-off) is shown as the solid line. Flutter occurs, for the uncontrolled aircraft, to the right of this line. The dashed line identifies a boundary to the left of which the FS control law should provide stability with ± 6 dB gain margins and ± 45° phase margins. In addition, to the left of this dashed boundary, the root mean square (rms) control deflection should be less than 15° and the rms control rate should be less than 740°/sec in the presence of random turbulence (Dryden spectrum with rms velocity of 12 ft/sec). The remaining curve defines a boundary to the left of which the FS control law should provide stability.

This paper presents results that show control law performance at the two points noted. Reference 24 gives more details about the FS design discussed here and also defines the performance over a range of flight conditions of a control law for which the overall gain is scheduled as a function of dynamic pressure.

The nominal design point, identified with a square, is at M=0.86 and an altitude of 15,000 ft. Note that the uncontrolled plant is unstable at this condition, which is at a dynamic pressure 16.5 percent above the open loop flutter point.

The point identified with a circle defines the flight condition at which constrained minimization techniques are employed to maximize control law robustness.

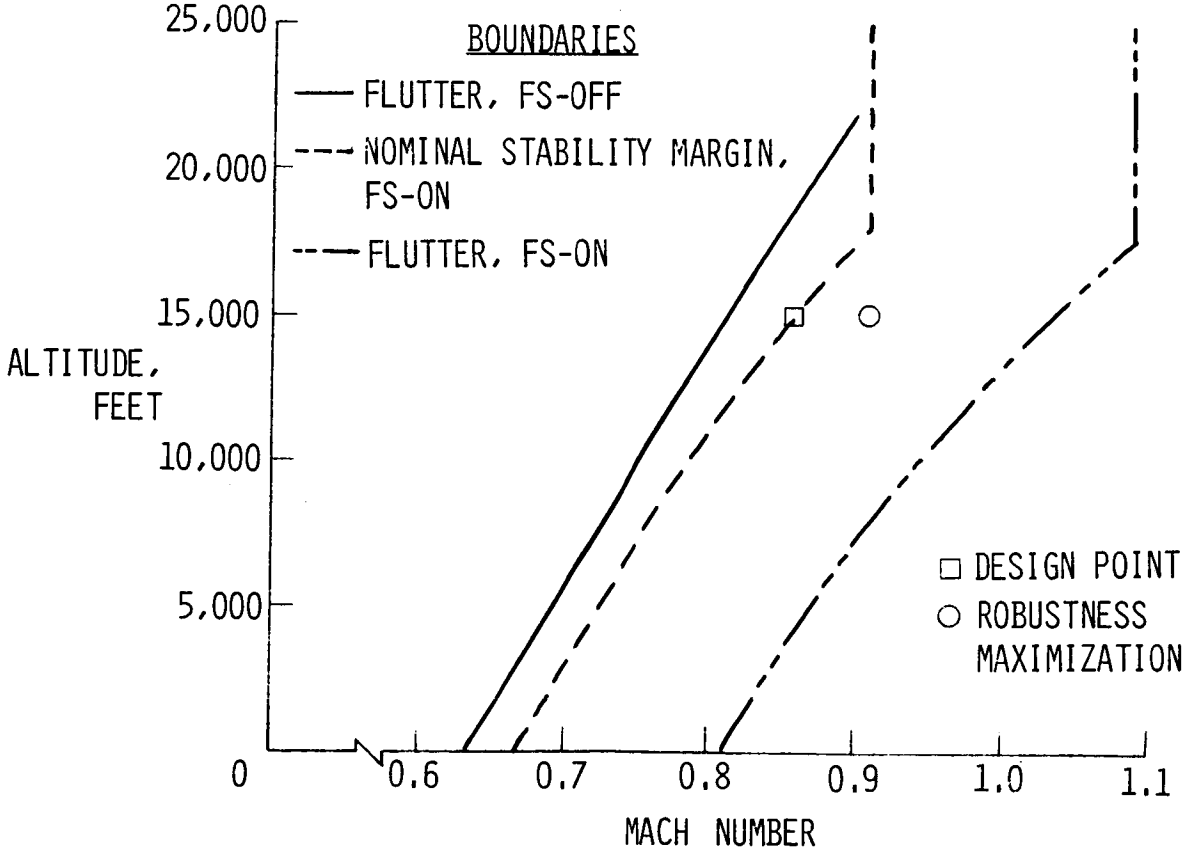

CONTROLLER DESIGN

Two control law design approaches were employed. In the first of these, optimal regulator theory was employed to determine a full-state feedback gain matrix. In this phase of the design the state weighting matrix was set to zero and the control weighting matrix was set to the identity. This choice of weighting matrices, plus the constraint that the closed-loop system be stable, results in the minimum control effort solution which stabilizes the system (Ref. 5). The controller also reflects unstable poles about the imaginary axis while leaving stable poles fixed. The next step in the design was to construct a steady-state Kalman estimator based upon the 12 ft/sec rms gust input and a nominal set of measurement error statistics. The robustness of the resulting LQG design was then improved by using the robustness recovery technique of adding fictitious noise at the input (Ref. 4). The ORACLS (Ref. 1) software was utilized to obtain the LQG designs. The 25th order controllers found were reduced to implementable sizes. The order reduction was accomplished by transforming the controller state space representation to block diagonal form and examining the poles, zeros, and residues of the full-order controller. Modal truncation was performed in the transformed domain to obtain candidate reduced-order controllers. It was found (Ref. 24) that the controller could be reduced from 25th order to 9th order with minimal degradation in controller performance.

The second design approach, which will be discussed after some specific LQG results are presented, made use of a nongradient-based, nonlinear programming algorithm (Refs. 25,26) to maximize robustness properties.

- MINIMUM CONTROL EFFORT LQ SOLUTION (ZERO STATE WEIGHTING)
- STEADY-STATE KALMAN ESTIMATOR
- DOYLE-STEIN ROBUSTNESS RECOVERY
- SELECTION OF REDUCED-ORDER CONTROLLER (9TH ORDER CHOSEN)
- ROBUSTNESS MAXIMIZATION

CLOSED-LOOP BLOCK DIAGRAM

This block diagram defines parameters that will be shown in subsequent figures to demonstrate controller performance. The output, y, is the FS sensor signal. G is the uncontrolled plant transfer function, y/u. The full model in frequency domain form (no s-plane approximation) was employed to perform a "one time" computation of G ($i\omega$) at a discrete set of frequencies. H, here and in the results to follow, is a reduced-order controller. The white-noise inputs included in the design process are gust (W_G), measurement (W_M) and control (W_U). Controllers were designed for a range of controller input noise intensities in order to determine an acceptable trade-off between robustness recovery, control power requirements and controller bandwidth. Results will be shown for two input noise intensity levels; zero and a "nominal" level selected as resulting in an acceptable design. The controller performance results are presented in terms of Nyquist plots which are polar plots of HG with the loop broken as indicated and with frequency as the independent variable.

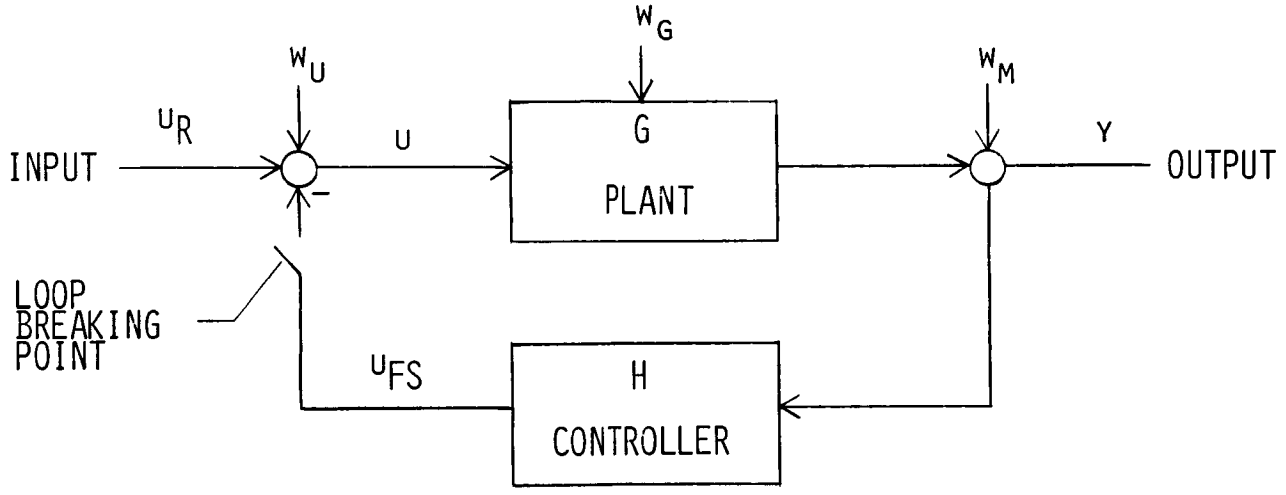

NYQUIST PLOT OF HG TRANSFER FUNCTION
(ZERO INPUT NOISE DESIGN)

This Nyquist plot is for a controller designed by applying LQG techniques with zero process noise intensity at the control input followed by controller order reduction (from 25th to 9th order). Since the uncontrolled plant is unstable with a complex conjugate pair of unstable poles, the Nyquist plot must, for closed—loop stability, encircle the -1 point once in a counterclockwise direction as ω varies from 0 to ∞. The arrow indicates the direction of increasing frequency. Gain margins of $\pm$ 6 dB are achieved. However, the 45° phase margin constraint is violated. Reference 24 contains additional data, such as the control power requirements and the frequencies corresponding to the gain margin and phase margin points.

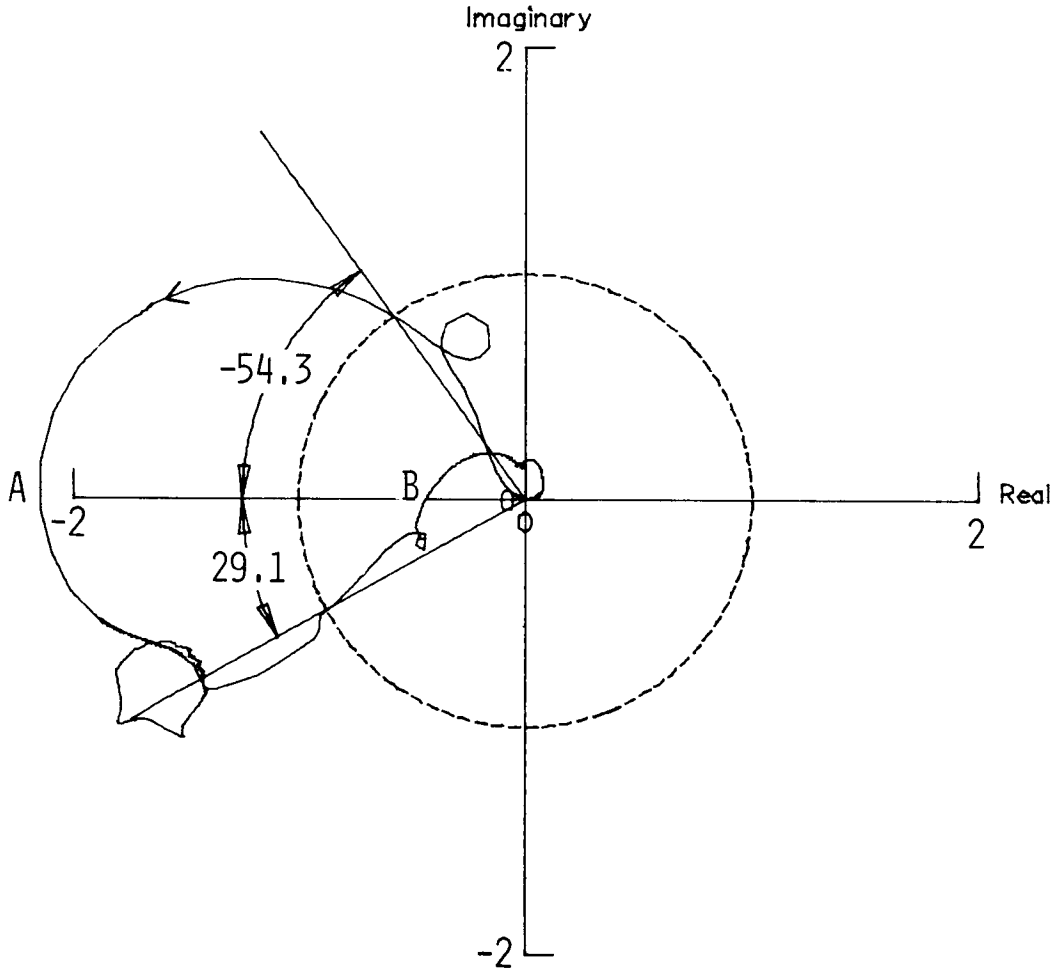

NYOUIST PLOT OF HG TRANFER FUNCTION
(NOMINAL INPUT NOISE DESIGN)

Additional full-order LQG controller designs were obtained with process noise intensity as a variable. Nyquist plots and controller Bode plots were examined for each of the resulting full-order controllers. A "nominal input noise" design was chosen which met the performance specifications, and order reduction techniques were employed to obtain an implementable controller (9th order). The Nyquist plot shown here, which is constructed by using the frequency domain evaluation model and the "nominal noise intensity" reduced-order controller, meets the gain margin and phase margin specifications. Both gain margins and phase margins are better than those achieved by using the "zero input noise intensity" controller of the previous figure. The rms control deflection and rate requirements of both controllers were within the constraints.

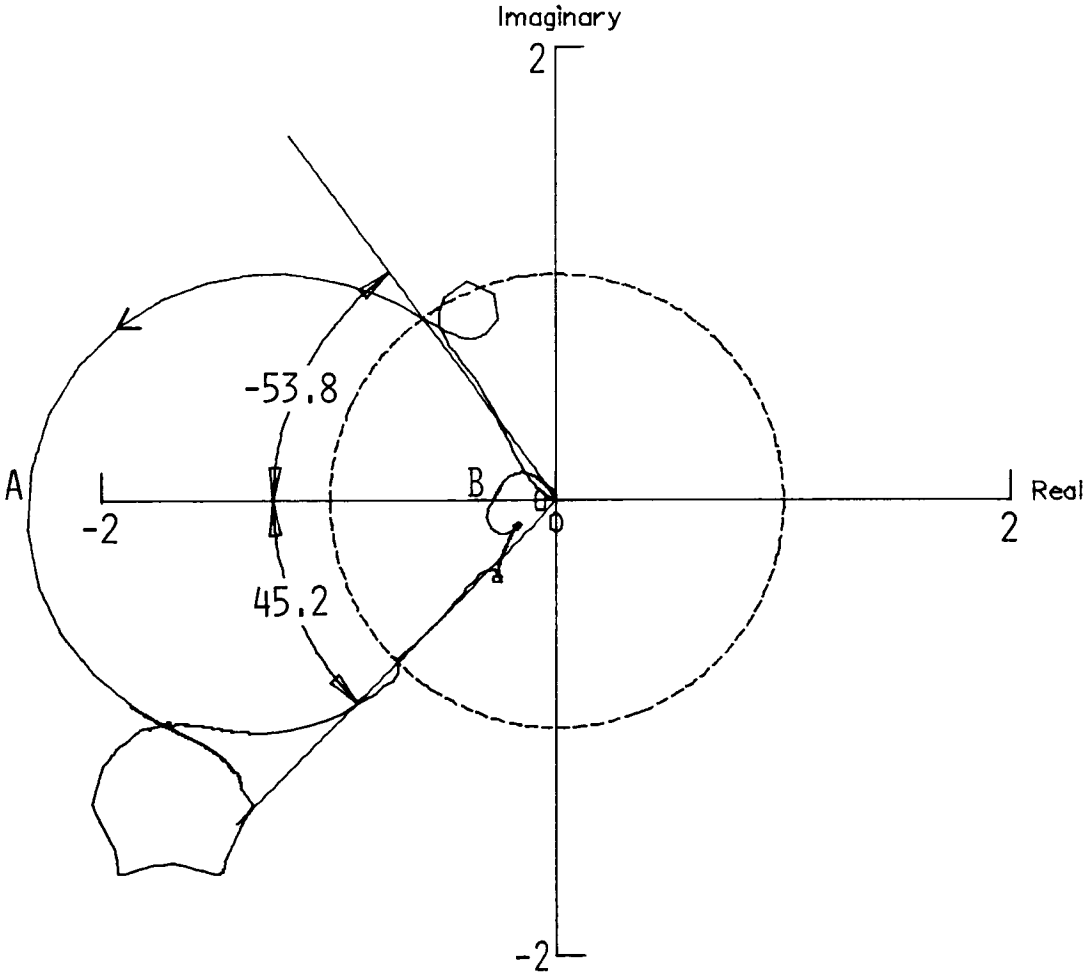

AMPLITUDE OF CONTROLLER TRANSFER FUNCTION VERSUS FREQUENCY

The phase margin and gain margin improvements that were obtained by increasing process noise at the input were not achieved without cost. A Bode plot of the "zero" and "nominal" input process noise controllers reveals that increasing the noise has degraded the controller high-frequency rolloff characteristics.

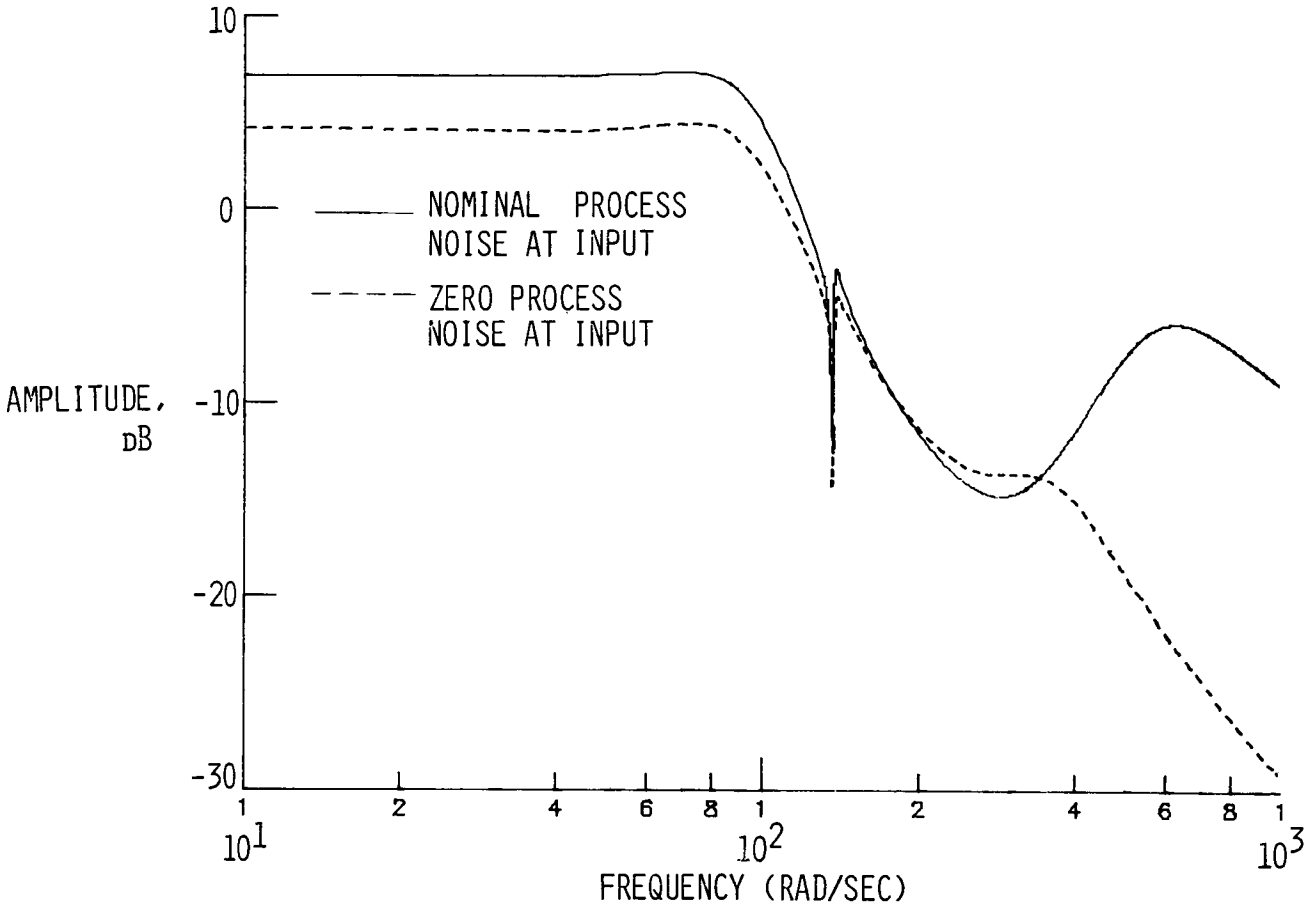

ROBUSTNESS MAXIMIZATION

An alternate design approach which allows explicit consideration of design criteria will now be described. The approach, which requires that the form of the control law be specified, is particularly applicable in modifying an existing control law when small changes occur in the plant or in satisfying criteria not fully considered in a previous design. Nongradient-based constrained minimization techniques are employed to maximize the minimum singular value of the return difference transfer function subject to explicit constraints on stability, gain margins, phase margins and control power requirements. A similar approach (Ref. 11), which employs a gradient-based optimizer, has been applied to improve the robustness of a lateral stability augmentation control law.

The method is applied to determine a controller for a flight condition having a Mach number of 0.91 and an altitude of 15,000 feet. The reduced-order controller found for the M = 0.86, 15,000-foot altitude flight condition was chosen to define the control law form and the initial values for the design variables. Nine of the controller coefficients were selected as design variables. Fixed-controller elements were lumped into a filter T(s). Stability was determined by computing the number of counterclockwise encirclements of the -1 point as ω varied from 0 to ∞. The phase margin requirements for this condition were relaxed to $\pm$ 40°.

In performing the constrained optimization, it was observed that control power requirements never reached their available limits. Control power constraints were, therefore, removed from the computations. This allowed the remaining constraints to be evaluated based solely upon the computations required for generation of Nyquist plots.

FIND VALUES FOR THE DESIGN VARIABLES, D_I, WHERE

$$\left(\frac{U_{FS}}{Y}\right) = D_1 \frac{(S+D_2)(S+D_3)}{(S^2+D_4 S+D_5)} \frac{(S^2+D_6 S+D_7)}{(S^2+D_8 S+D_9)} T(S)$$

AND T(S) IS A FIXED FILTER

SUCH THAT

- MINIMUM SINGULAR VALUE IS MAXIMIZED
- CONTROL POWER CONSTRAINTS ARE SATISFIED
- +6DB $\leq$ GAIN MARGIN $\leq$ -6DB
- 40° $\leq$ PHASE MARGIN $\leq$ -40°

NYQUIST PLOTS OF HG TRANSFER FUNCTION
(M = 0.91, H = 15,000 FEET)

The initial controller stabilized the system but gain margin constraints (± 6 dB) and phase margin constraints (± 40°) were violated. The minimum singular value is indicated by the heavy line. The constrained optimization solution has a 26 percent larger minimum singular value; gain margin and phase margin constraints are satisfied to within a 2.5 percent tolerance. Control power requirements (rms requirements) are also reduced with the optimized controller.

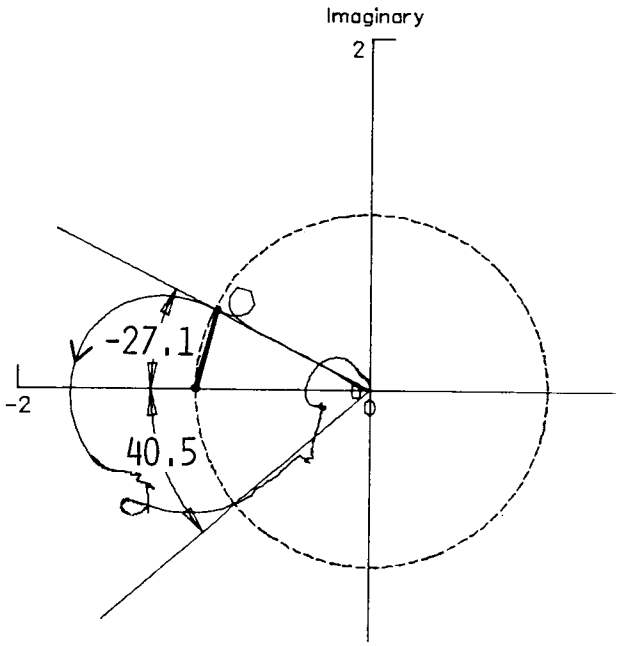

INITIAL CONTROLLER

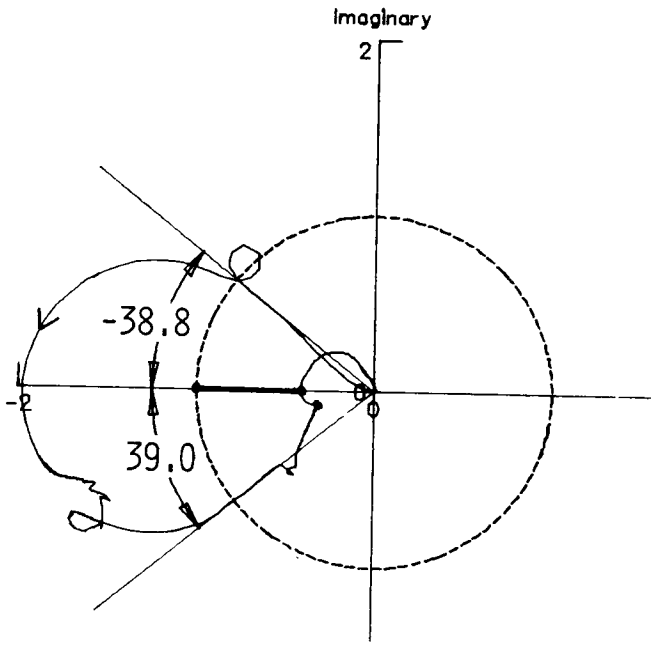

OPTIMIZED CONTROLLER

SUMMARY

Coupling the ISAC program (for definition of plant design and evaluation models) with the ORACLS LQG methodology provided an effective tool for design of full-order controllers. Addition of process noise at the input allowed stability margin criteria to be met. The rms control deflection and rate requirements were also within their constraints. Controller order reduction from 25th to 9th was successfully accomplished with minimal sacrifice in controller performance.

Robustness maximization using nongradient-based constrained optimization techniques substantially increased the minimum singular value of the return difference transfer function for an off-nominal flight condition. Stability was determined at each iteration by computing the number of counterclockwise encirclements of the -1 point as ω varied from 0 to ∞.

New FS control laws will be designed for both symmetric and antisymmetric degrees of freedom when the mathematical model of the ARW-2 is updated.

- 9TH ORDER CONTROLLER DEVELOPED USING LQG TECHNIQUES AND ORDER REDUCTION ACHIEVED DESIGN OBJECTIVES
- ROBUSTNESS MAXIMIZATION USING NONGRADIENT-BASED CONSTRAINED OPTIMIZATION TECHNIQUES INCREASED MINIMUM SINGULAR VALUE SUBSTANTIALLY
- DESIGN WILL BE REPEATED FOR BOTH SYMMETRIC AND ANTISYMMETRIC FLUTTER WHEN UPDATED STRUCTURAL MODEL IS COMPLETED

REFERENCES

1. Armstrong, Ernest S.: ORACLS - A Design System for Linear Multivariable Control. Marcel Dekker, Inc., c.1980.

2. Mahesh, J. K.; Stone, C. R.; Garrard, W. L.; and Hausman, P. D.: Active Flutter Control for Flexible Vehicles. NASA CR-159160, November 1979.

3. Gangsaas, Dagfin; and Ly, Uy-Loi: Application of Modified Linear Quadratic Gaussian Design to Active Control of a Transport Airplane. AIAA Paper No. 79-1746, August 1979.

4. Doyle, J. C.; and Stein, G.: Robustness with Observers. IEEE Transactions on Automatic Control, August 1979.

5. Kwakernaak, Huibert; and Sivan, Raphael: Linear Optimal Control Systems. Wiley-Interscience, c.1972.

6. Mukhopadhyay, V.; Newsom, J. R.; and Abel, I.: A Direct Method for Synthesizing Low-Order Optimal Feedback Control Laws with Application to Flutter Suppression. AIAA Paper No. 80-1613, August 1980.

7. Schy, A. A.: Nonlinear Programing in the Design of Control Systems with Specified Handling Oualities. Proceedings of 1972 IEEE Conference on Decision and Control, New Orleans, LA, December 1972.

8. Schy, A. A.; Adams, William M., Jr.; and Johnson, K. G.: Computer-Aided Design of Control Systems to Meet Many Requirements. NATO AGARD Conference Proceedings No. 137 on Advances in Control Systems, 1973.

9. Knox, J. R.; and McCarty, J. M.: Algorithms for Computation of Optimal Constrained Output Feedback for Linear Multivariable Systems. AIAA Paper No. 78-1290, August 1978.

10. Adams, William M., Jr.; and Tiffany, Sherwood H.: Control Law Design to Meet Constraints Using SYNPAC--Synthesis Package for Active Controls. NASA TM-83264, January 1982.

11. Newsom, Jerry R.; and Mukhopadhyay, V.: The Use of Singular Value Gradients and Optimization Techniques to Design Robust Controllers for Multiloop Systems. AIAA Paper No. 83-2191, August 1983.

12. Peele, Ellwood L.; and Adams, William M., Jr.: A Digital Program for Calculating the Interaction Between Flexible Structures, Unsteady Aerodynamics, and Active Controls. NASA TM-80040, January 1979.

13. Albano, E.; and Rodden, W. P.: A Doublet Lattice Method for Calculating Lift Distributions on Oscillating Surfaces in Subsonic Flows. AIAA Journal, Vol. 7, No. 2, February 1969, pp. 279-285.

14. Giesing, J. P.; Kalman, T. P.; and Rodden, W. P.: Subsonic Unsteady Aerodynamics for General Configurations. AFFDL-TR-71-5, November 1971.

15. Rodger, Kenneth L.: Airplane Math Modeling Methods for Active Control Design. AGARD CR-228, August 1977.

16. Jones, R. T.: The Unsteady Lift of a Wing of Finite Aspect Ratio. NACA Rept. 641, 1940.

17. Vepa, R.: Finite State Modeling of Aeroelastic Systems. Ph.D. Dissertation, Department of Applied Mechanics, Stanford University, June 1975.

18. Edwards, John W.: Unsteady Aerodynamic Modeling and Active Aeroelastic Control. NASA CR-148019, 1977.

19. Dunn, H. J.: An Analytical Technique for Approximating Unsteady Aerodynamics in the Time Domain. NASA TP-1738, November 1980.

20. Boeing Commercial Aircraft Company Staff: Integrated Application of Active Controls (IAAC) Technology to an Advanced Subsonic Transport Project - Wing Planform Study and Final Configuration Selection. NASA CR-165630, June 1981.

21. Military Specifications - Flying Qualities of Piloted Airplanes. MIL-F-8785C, November 5, 1980. (Superseding MIL-F-8785B, August 7, 1969.)

22. Schwanz, Robert C.: Consistency in Aircraft Structural and Flight Control Analysis. AGARD CR-228, August 1977.

23. Newsom, J. R.; Pototsky, Anthony S.; and Abel, I.: Design of the Flutter Suppression System for DAST ARW-1-1R - A Status Report. NASA TM-84642, March 1983.

24. Adams, William M.; and Tiffany, Sherwood H.: Design of a Candidate Flutter Suppression Control Law for DAST ARW-2. AIAA Paper No. 83-2221, August 15-17, 1983.

25. Olsson, D. M.: A Sequential Simplex Program for Solving Minimization Problems. Journal of Quality Technology, Vol. 6, No. 1, January 1974, pp. 53-57.

26. Olsson, Donald M.; and Nelson, Lloyd S.: The Nelder-Mead Simplex Procedure for Function Minimization. Technometrics, Vol. 17, No. 1, February 1975.